# AB INITIO MODELLING OF NONLINEAR ELASTOPLASTIC PROPERTIES OF DIAMOND-LIKE C, SiC, Si, Ge CRYSTALS UPON LARGE STRAINS

## R.S. Telyatnik[1,2*] , A.V. Osipov[1-3], S.A. Kukushkin[1-4]

[1]Institute of Problems of Mechanical Engineering of Russian Academy of Sciences,

Bolshoy pr. 61, V.O., St. Petersburg, 199178, Russia

[2]Saint-Petersburg Academic University of Russian Academy of Sciences,

Hlopina ul. 8/3, St. Petersburg, 194021, Russia

[3]St. Petersburg National Research University of Information Technologies, Mechanics, and Optics,

Kronverkskii pr. 49, St. Petersburg, 197101, Russia

[4]Peter the Great Saint-Petersburg Polytechnic University,

Politekhnicheskaya ul. 29, St.-Petersburg, 195251, Russia

*e-mail: statphys@ya.ru

**Abstract.** 5-th order nonlinear elastic properties of diamond-like single crystals are investigated by computational quantum chemistry, brief introduction to which is supplied. DFT LDA and DFT GGA methods are used to calculate curves of stress dependency on tensile, compressive and shear strains with account of structure relaxation in huge strain range until irreversible deformation occurs at strength limit. Limits of linear elastic proportionality, maximal stresses, regions of necking non-plastic creep are indicated. Relations between linear limits of axial and shear stresses, determined by bilinear approximations of the curves, are represented by Hill's surface as an estimation of plastic anisotropy. Elastic constants are calculated both for finite and small strains. Polynomial approximations are made for dependencies of full energy, crystal volume, Poisson coefficient on strain. Determined parameters can be used for finite-element modelling in mechanical engineering and for reexamination of indentation tests.

## 1. Introduction
Development of advanced semiconductor (Si, SiC, Ge) engineering requires new detectors, generators, microelectromechanical systems (MEMS) and other devices using such phenomena like magneto- and electrostriction, piezoelectric, piezoresistive and other effects conjugated with deformation [1, 2]. Nonlinear elastic and plastic material properties are required and essential for finite-element modeling (FEM) of large deformations in mechanical engineering, e.g. for modeling indentation test, which can help to extract elastic-plastic properties from corresponding experiment [3]. However, there is usually a lack of experimental data on elastic constants for new materials, while for the majority of anisotropic materials, there is no information about limits of linear proportionality, nonlinearity, yield, creep, and strength at failure upon large strains, both axial and shear. Moreover, one cannot simply extract by experiment nonlinear elastic properties of non-ideal crystals exhibiting also plastic behavior. That is why over the last decades the interest to chemical calculations predicting elastic linear and nonlinear properties up to structural transformations under high pressure (usually volumetric and not directional) has grown significantly for materials with an absence of

experimental data. Methods of computational quantum chemistry [4, 5, 6], known as *ab initio* methods (Latin "from first-principles"), are very attractive in this sense, because they don't require any empirical data on atomic potentials, but they rely on different approximations of many-electron problem. The most rapid and popular solution of the problem is Density Functional Theory (DFT) in Local Density Approximation (LDA) or Generalized Gradient Approximation (GGA) [7, 8]. Pseudopotential approximations of core (non-valence) electrons are usually incorporated.

   In this paper, it is presented a brief introduction to essentials of *ab initio* methods and calculation of elastic constants of crystals. For diamond C and diamond-like semiconductors, such as silicon Si, germanium Ge, silicon carbide SiC of sphalerite polytype, stress dependencies on large axial and shear strains are calculated for absolute zero temperature by DFT LDA and DFT GGA pseudopotential methods using ABINIT software [8]. Effective for large strains elastic constants and nonlinear stress-strain dependencies are determined along with linear proportionality limits, maximal stresses, necking regions (non-plastic creep) and strength limits. Anisotropic elastic constants are also calculated by method of response functions to small perturbations of atoms positions for comparison with the finite strain method. Correlation between computed stress-strain curves representing pure nonlinear elastic behavior until strength limit and real curves incorporating also plastic strain is discussed. Comparison with exterior experimental data is provided.

## 2. Calculation of strain related material constants

Deformation of a crystal is determined by a transformation of undeformed Bravais lattice vectors $\vec{b}_i$ to deformed ones $\vec{b}_i'$. In case of small deformation, the transformation is expressed by strain tensor $\varepsilon$ ($\delta$ – Kronecker delta, Einstein's summation rule over repeated indices is used hereafter):

$$b_{i\alpha}' = \left( \delta_{\alpha\beta} + \varepsilon_{\alpha\beta} \right) b_{i\beta} \ , \ \ \alpha, \beta = x, y, z \ , \ \ i = 1, 2, 3 . \tag{1}$$

Hook's law for anisotropic materials relates stress to strain via 4-rank tensor of stiffnesses. This relation can be expressed in matrix form by Voight notations with indices 1,…, 6 corresponding to xx, yy, zz, yz, xz, xy, except for strains $\varepsilon_4 = 2\varepsilon_{yz}$, $\varepsilon_5 = 2\varepsilon_{xz}$, $\varepsilon_6 = 2\varepsilon_{xy}$ [10]:

$$\sigma_{\alpha\beta} = c_{\alpha\beta\mu\nu} \varepsilon_{\mu\nu} \ (\alpha, \beta, \mu, \nu = x, y, z) \ \leftrightarrow \ \sigma_i = c_{ij} \varepsilon_j \ (i, j = 1, ..., 6) . \tag{2}$$

Cubic symmetry keeps only 3 independent elastic constants:

$$\begin{pmatrix} \sigma_{xx} \\ \sigma_{yy} \\ \sigma_{zz} \\ \sigma_{yz} \\ \sigma_{xz} \\ \sigma_{xy} \end{pmatrix} = \begin{pmatrix} c_{11} & c_{12} & c_{12} & 0 & 0 & 0 \\ c_{12} & c_{11} & c_{12} & 0 & 0 & 0 \\ c_{12} & c_{12} & c_{11} & 0 & 0 & 0 \\ 0 & 0 & 0 & c_{44} & 0 & 0 \\ 0 & 0 & 0 & 0 & c_{44} & 0 \\ 0 & 0 & 0 & 0 & 0 & c_{44} \end{pmatrix} \begin{pmatrix} \varepsilon_{xx} \\ \varepsilon_{yy} \\ \varepsilon_{zz} \\ \gamma_{yz} \\ \gamma_{xz} \\ \gamma_{xy} \end{pmatrix} , \ \gamma_{\alpha\beta} = 2\varepsilon_{\alpha\beta} . \tag{3}$$

In this case, engineering Young's modulus $E$, Poisson coefficient $v$ and shear modulus $G$ can be expressed from inverse stiffness matrix, i.e. matrix of compliances $s = c^{-1}$:

$$E \equiv \frac{1}{s_{11}} = \frac{c_{11}^2 + c_{11}c_{12} - 2c_{12}^2}{c_{11} + c_{12}}; \ v \equiv -\frac{s_{12}}{s_{11}} = \frac{c_{12}}{c_{11} + c_{12}}; \ G \equiv \frac{1}{s_{44}} = c_{44} \tag{4}$$

   To calculate elastic constants of a crystal, it is enough to obtain second derivatives on strains of full energy (per unit volume) of a primitive cell in small strain limit of harmonic approximation. In the nonlinear theory of elasticity and finite strains [11, 13] the strain energy

can be expanded with higher order elastic constants (using the Lagrangian definition of strain tensor):

$$\Delta U^{strain} = \frac{1}{2} c_{ij} \varepsilon_i \varepsilon_j + \frac{1}{6} c_{ijk} \varepsilon_i \varepsilon_j \varepsilon_k + ... \;,\;\; c_{ij} = \left. \frac{\partial^2 U}{\partial \varepsilon_i \partial \varepsilon_j} \right|_{\varepsilon=0} \;,\;\; c_{ijk} = \left. \frac{\partial^3 U}{\partial \varepsilon_i \partial \varepsilon_j \partial \varepsilon_k} \right|_{\varepsilon=0} \;,\; ... \tag{5}$$

Second and third order elastic constants can be determined experimentally by sound propagation [14, 15] as well as by *ab initio* methods [16]. In this paper, for big strains up to phase transformation (leading to new local minimum of the energy), the total energy has been calculated *ab initio* and approximated with 5th order polynom. In general anisotropic case of triclinic symmetry, there are 21 $c_{ij}$ independent constants, 56 $c_{ijk}$, 126 4th order $c_{ijkl}$, 352 5th order $c_{ijkl}$ constants. In cubic crystals, there are 6 or 8 independent $c_{ijk}$ constants depending on symmetry (6 for diamond-like one: $c_{111}$, $c_{112}$, $c_{123}$, $c_{456}$, $c_{144}$, $c_{166}$). Nevertheless, determination of such large amount of coefficients to describe required 5th order anharmonicity is inefficient. In mechanical applications, it is much simpler to use approximations of Hook's formula with some functional dependency of $c_{ij}(\varepsilon_k)$ on strain. For diamond-like crystals we have made simple approximations to dependencies of 3 engineering moduli (Young modulus, Poisson coefficient, shear modulus) on "true" logarithmic Hencky axial strain (and angular shear strain) for ability to use them in finite-element calculations, which integrate small deformations upon loading [17]:

$$\varepsilon_{xx}^{engineer} = \frac{\Delta L}{L} \;;\;\; \varepsilon_{xx}^{true} = \int_{L_0}^{L_0 + \Delta L} \frac{dL}{L} = \ln \left( 1 + \varepsilon_{xx}^{engineer} \right). \tag{6}$$

Experimental data on true stress (per area of deformed body, not undeformed one) relative to true strain are usually supposed as input in FEM software like ANSYS. Poisson coefficient is considered here as relation of true strains. Logarithmic strains cause additional tension-compression asymmetry of a stress-strain curve.

     *Ab initio* perturbation methods, such as Density Functional Perturbation Theory (DFPT) [18, 19] realized in ABINIT package, allow to calculate system response not only on atomic displacements, but on external electric and magnetic fields as well. Energy second derivatives on such perturbations, including mixed ones, give dielectric permittivity tensor, piezoelectric constants, and allow to calculate phonon and Raman spectra. Diatomic diamond-like (i.e. sphalerite type) crystals have only one nonzero component $e_{14}$ of piezoelectric coefficients tensor. In mechanic sense, response function, i.e. lattice Green's function of solid state theory [20], in the limits of spatial continuity and zero-frequency phonons, reduces to elastic static tensorial Green's function, which characterize displacement field caused by unit force. In this paper, we calculated $c_{ij}$ stiffness coefficients in the limit of small strains by response function method to be assured in consistency with used finite strains method.

     Nonlinearity of stress-strain curve may represent not only reversible nonlinear elasticity, but also irreversible plastic deformations (see the theory of plasticity [21-23]). Elastoplastic stress-strain curve usually have simple bilinear law described by elastic modulus $E_1$ and tangent modulus $E_2$ ($\Theta(\varepsilon)$ - Heaviside function):

$$\sigma_{xx}(0 < \varepsilon_{xx} < \varepsilon_C) = E_1 \varepsilon_{xx} \Theta(\varepsilon_Y - \varepsilon_{xx}) +$$
$$+ \left( E_2 \varepsilon_{xx} + \left( E_1 - E_2 \right) \varepsilon_{Y1} \right) \Theta(\varepsilon_{xx} - \varepsilon_Y) \;,\; E_2 = \frac{\sigma_C - E_1 \varepsilon_Y}{\varepsilon_C - \varepsilon_Y} \tag{7}$$

Here, $\varepsilon_Y$ is the yield limit above which residual plastic strain remains after unloading, $\sigma_C$ is maximal stress at strain $\varepsilon_C$, above which response stress doesn't increase, and the body undergo creep elongation under constant pressure $\sigma_C$ until fracture or structural transformation occurs at some ultimate strain $\varepsilon_U$. [23]). In single crystals, plasticity is caused mostly by formation and movement of dislocations along slip planes and by formation of other lattice defects and grains

in polycrystals and nanocrystalline materials [24, 25]. Dislocations, as quite big strain discontinuities, may be formed either in linear or nonlinear range of elasticity [26]. In the first case, the yield limit is lower than the limit of linear proportionality in pure nonlinear elasticity, otherwise in the second case. One cannot simply indicate the yield limit in the nonlinear range of stress-strain curve without unloading. In our *ab initio* calculations, nonlinear dependencies of stress on axial and shear strain (Figs. 1 – 9) don't exhibit plastic deformation until strength limit $\varepsilon_U$ is reached (see the results chapter), but the linear proportionality limits obtained by the bilinear approximations of the curves may serve as comparative limited estimations of the yield limits.

The yield stresses for axial and shear strains together allow us to understand at what moment plastic deformation starts during arbitrary complex loading. The von Mises criterion for the onset of plasticity in isotropic medium was first generalized for orthotropic case by Hill [23, 27], who predicts plastic deformation outside the limiting 6-dimensional Hill's surface in the space of three axial and three shear stresses:

$$F(\sigma_{yy} - \sigma_{zz})^2 + G(\sigma_{zz} - \sigma_{xx})^2 + H(\sigma_{xx} - \sigma_{yy})^2 + 2L\sigma_{yz}^2 + 2M\sigma_{xz}^2 + 2N\sigma_{xy}^2 \geq 1;$$

$$F = \left(-\sigma_{Y,xx}^{-2} + \sigma_{Y,yy}^{-2} + \sigma_{Y,zz}^{-2}\right)\big/2;$$

$$G = \left(\sigma_{Y,xx}^{-2} - \sigma_{Y,yy}^{-2} + \sigma_{Y,zz}^{-2}\right)\big/2; \tag{8}$$

$$H = \left(\sigma_{Y,xx}^{-2} + \sigma_{Y,yy}^{-2} - \sigma_{Y,zz}^{-2}\right)\big/2;$$

$$L = \sigma_{Y,yz}^{-2}\big/2; \; M = \sigma_{Y,xz}^{-2}\big/2; \; N = \sigma_{Y,xy}^{-2}\big/2.$$

The Hill's criterion is supported, for example, by ANSYS package of FEM analysis. Subsequently, this criterion also got various modifications and generalizations [28, 29]. In crystals of cubic symmetry, the elastic-plastic law is the same for different axial components (with a possible difference between tension and compression), and the same for different shear components, however, the isotropic ratios between axial and shear components is no longer satisfied – namely, the isotropic ratio between elastic moduli,

$$G = \frac{E}{2(1+\nu)} \;\; \Leftrightarrow \;\; c_{44} = \frac{c_{11} - c_{12}}{2} \;\; \text{(elastic isotropy)}, \tag{9}$$

and the condition of spherical symmetry of Mises surface:

$$h \equiv \left|\frac{\sqrt{3}\sigma_{Y,xy}}{\sigma_{Y,xx}}\right| = 1 \;\; \text{(plastic isotropy)}. \tag{10}$$

The 2D-projections of Hill's surfaces based on calculated linear proportionality limits (not directly yield limits, as discussed above) are presented on Fig. 10.

Since our paper is designed for mechanical engineers, we ought to provide hereafter brief introduction to the essentials of computational quantum chemistry.

## 3. Essentials of ab initio methods

Basic concept of quantum mechanics is wave function, characterizing state of a system depending on time and particles coordinates. It is possible to calculate wave function only for very simple systems, while for complex systems it is impossible in principle, so different approximations for many-body problem are used. In ordinary case, exploited by the theory of chemical binding, the Born-Oppenheimer adiabatic approximation is supposed by separating wave functions of atomic nucleus and electrons, since a motion of nucleus is much slower than that of electrons.
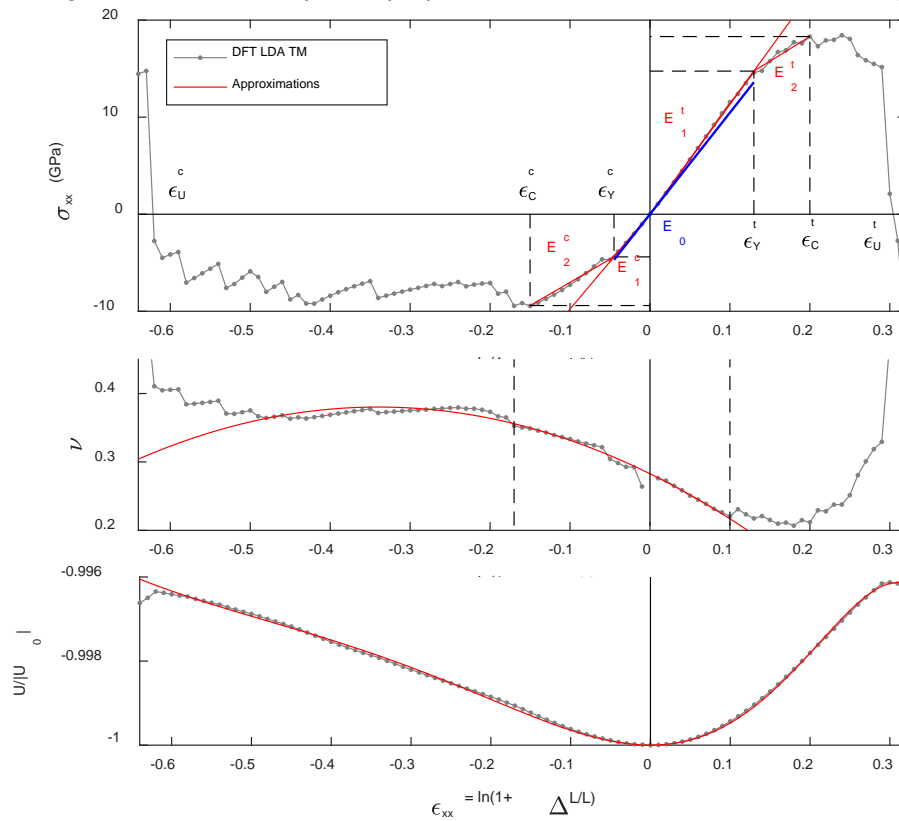
**Fig. 1.** Computed axial deformation of Ge. Stress, Poisson coefficient and relative total energy versus logarithmic strain.
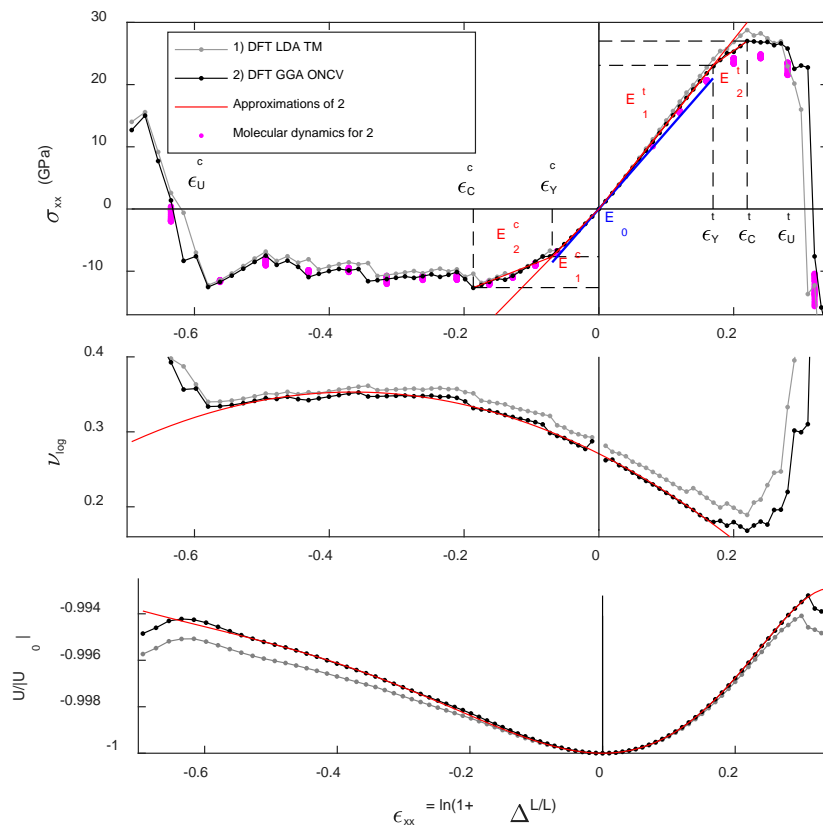


**Fig. 2.** Computed axial deformation of Si. Stress, Poisson coefficient and relative total energy versus logarithmic strain.
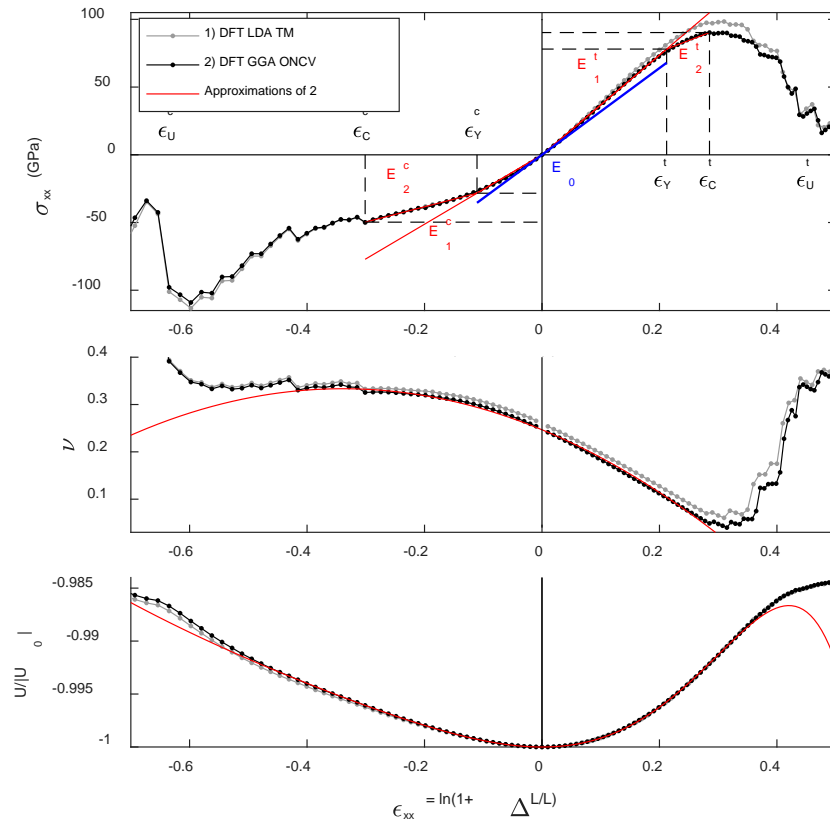
**Fig. 3.** Computed axial deformation of SiC. Stress, Poisson coefficient and relative total energy versus logarithmic strain.



**Fig. 4.** Computed axial deformation of C. Stress, Poisson coefficient and relative total energy versus logarithmic strain.
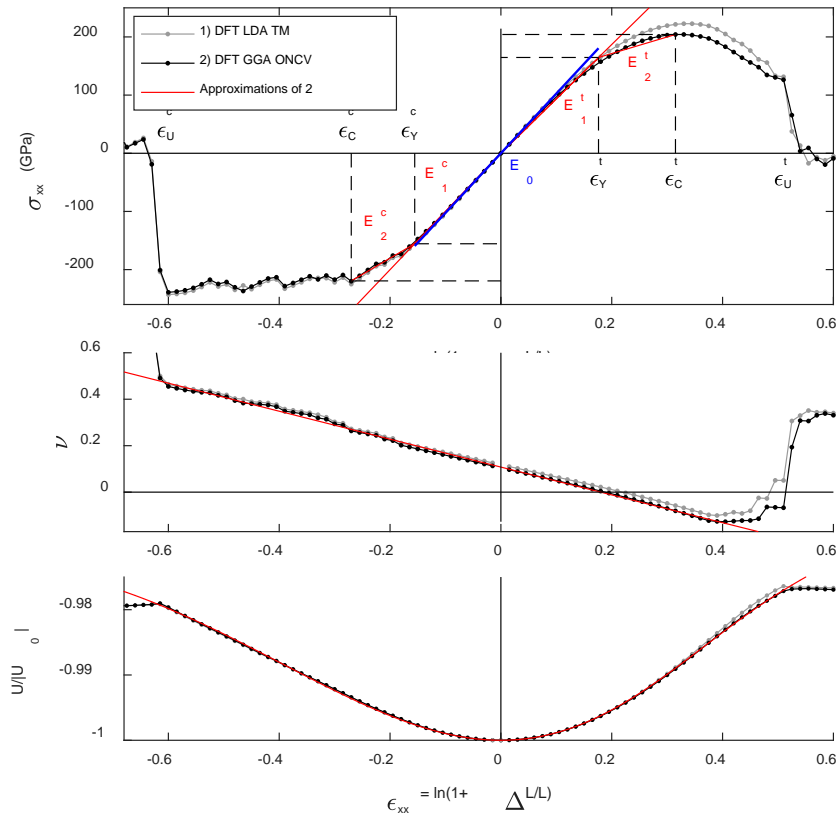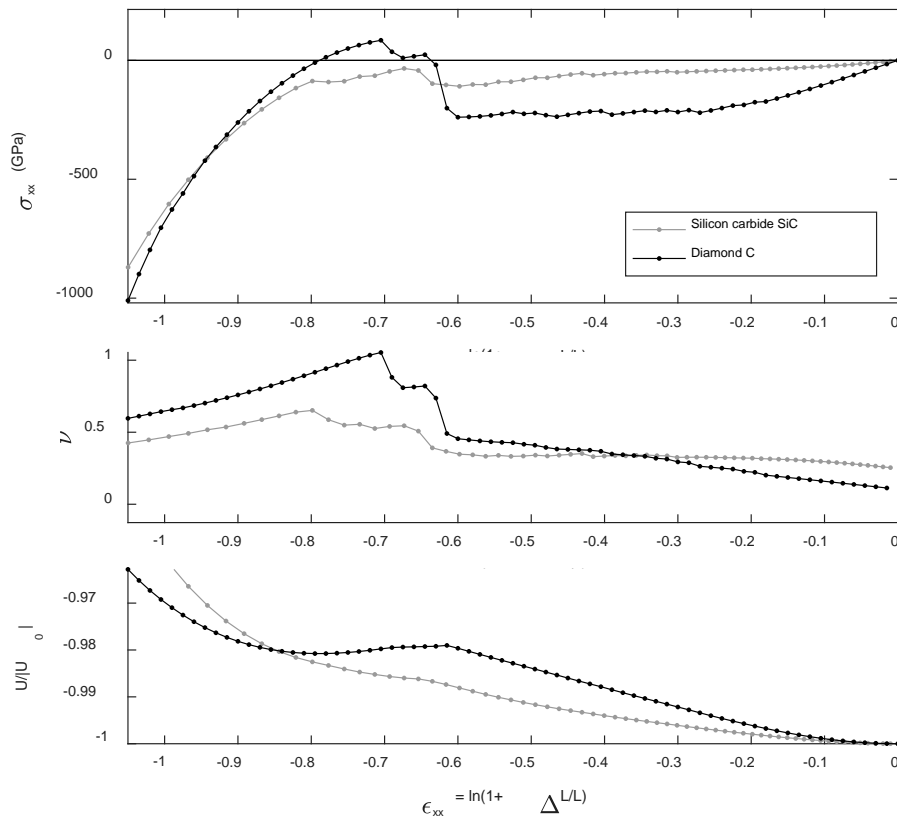
**Fig. 5.** Hyperelastic behavior upon big axial compression for all considered diamond-like crystals exemplified by C and SiC.



**Fig. 6.** Computed shear deformation of Ge. Stress, relative volume and relative total energy versus angle.

*R.S. Telyatnik, A.V. Osipov, S.A. Kukushkin*



**Fig. 7.** Computed shear deformation of Si. Stress, relative volume and relative total energy versus angle.
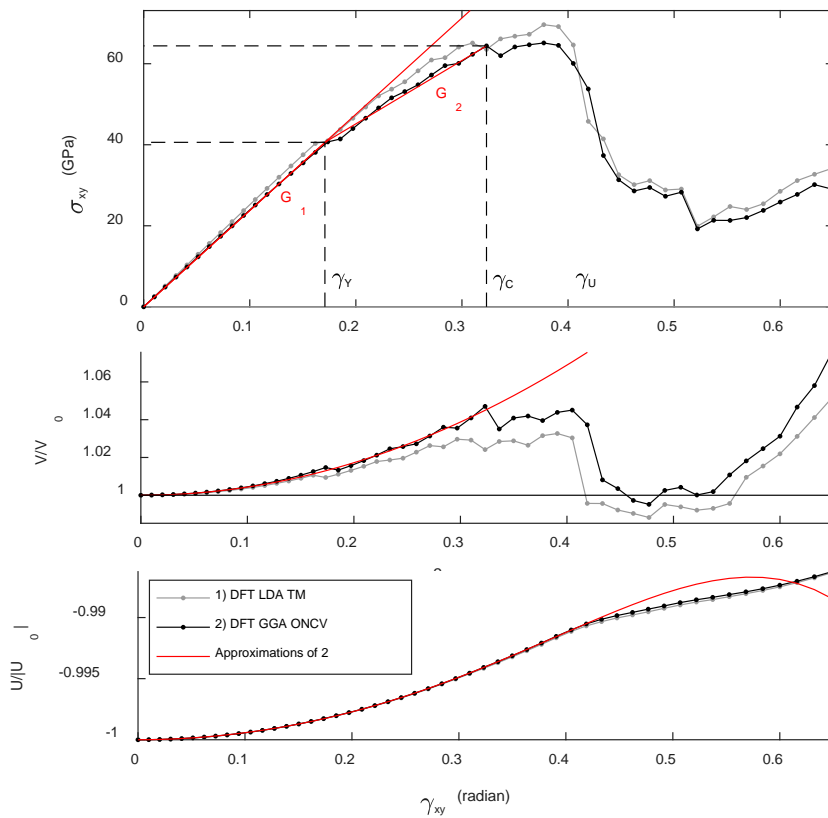


**Fig. 8.** Computed shear deformation of SiC. Stress, relative volume and relative total energy versus angle.

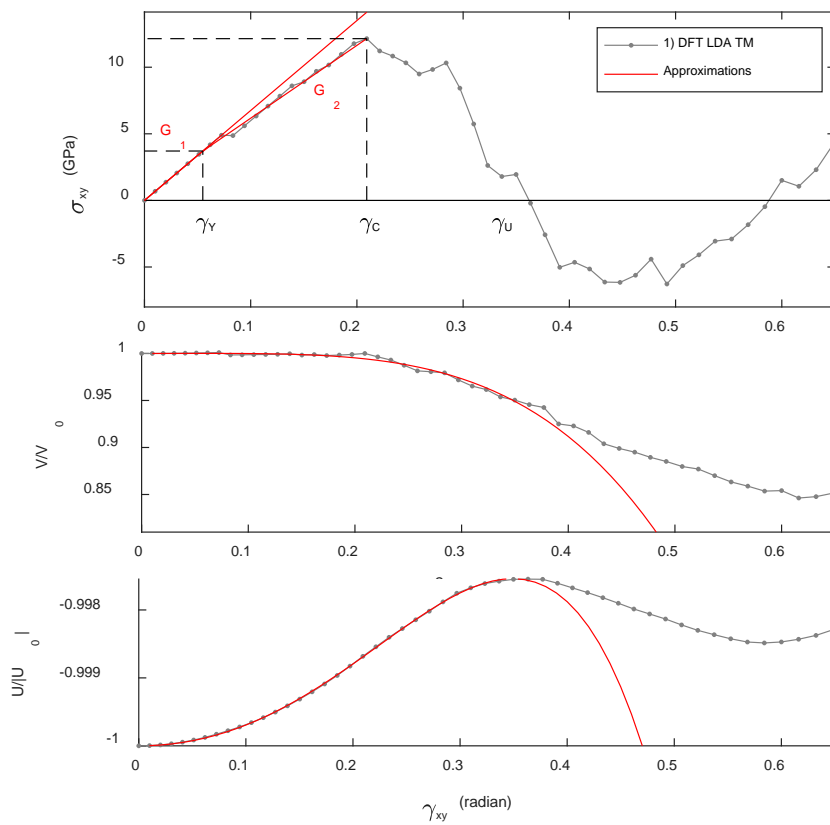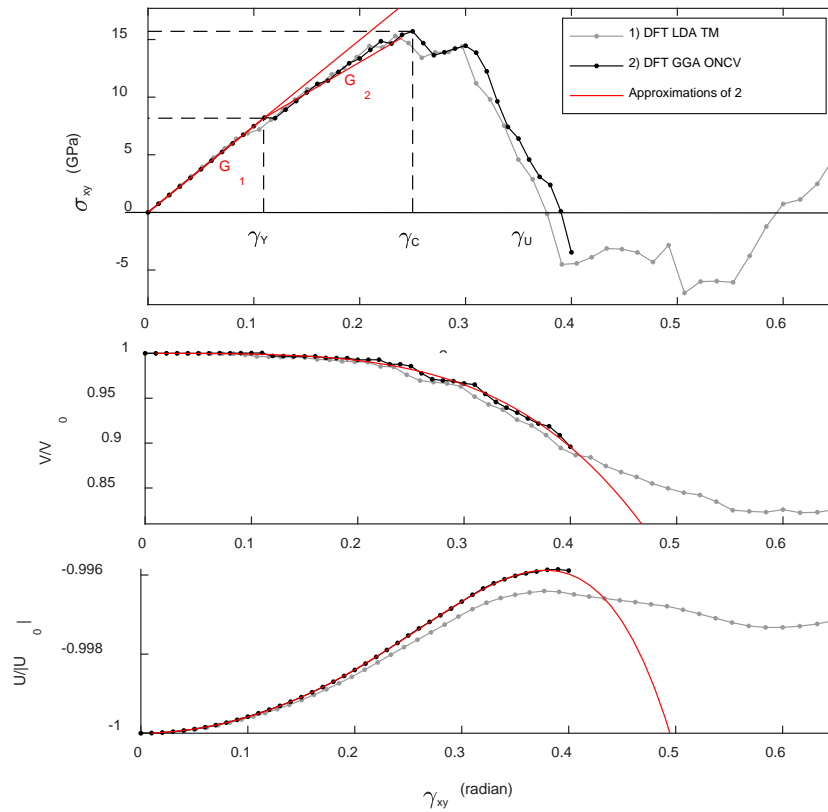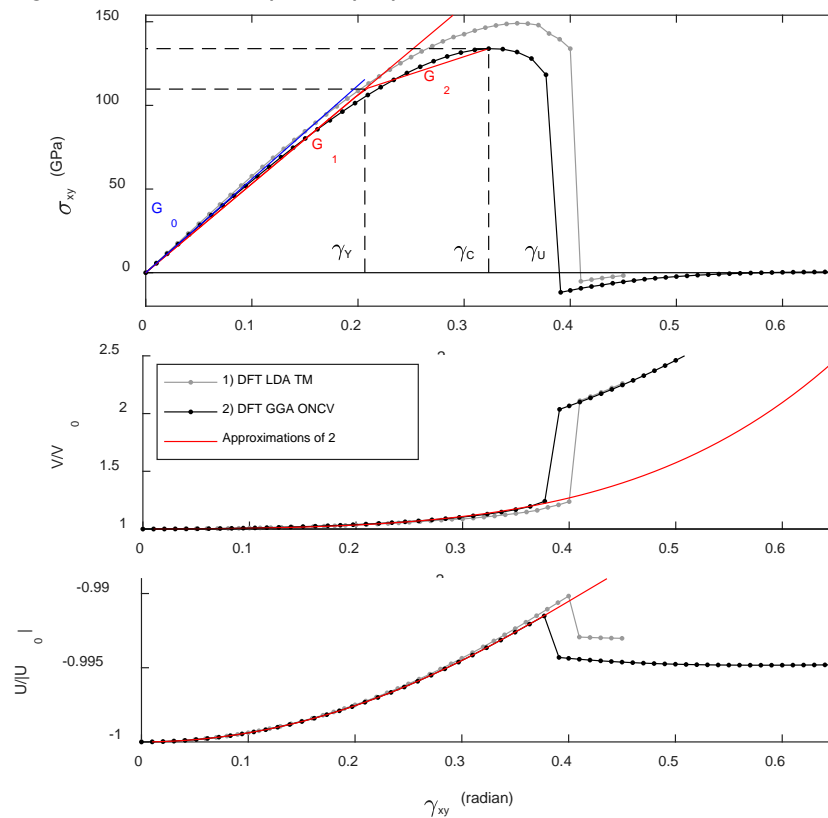**Fig. 9.** Computed shear deformation of C. Stress, relative volume and relative total energy versus angle.
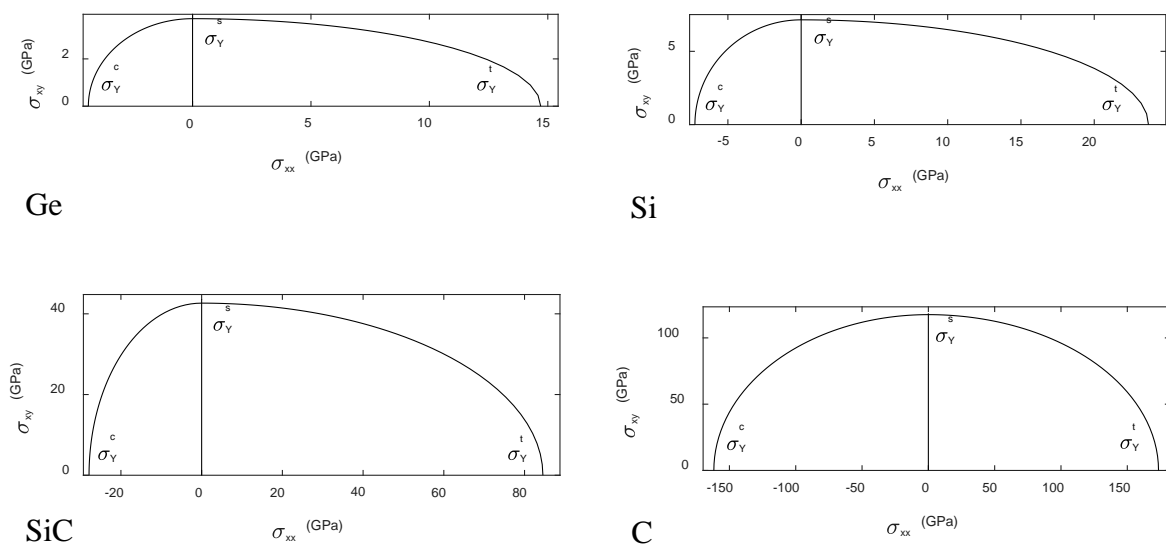


**Fig. 10.** Hill's surfaces (as relation between stress limits of linearity) in projection on the semi-plane ($\sigma_{xx}, \sigma_{xy} \geq 0$) for different crystals (by averaged results of DFT LDA TM and DFT GGA ONCV calculations).

Further approaches consider many-electron problem. It is usually treated by Self-Consistent Field (SCF) theory, which resolves into computation of independent electrons in a mean field of other particles. Such approaches are Hartee-Fock method and Kohn-Sham method. The first one solves Schrödinger equation via formalism of multi-fermion wave

functions factorized in form of Slater determinant accounting Pauli exclusion principle. The second one is the DFT method (based on Hohenberg-Kohn theorems) introducing formalism of electronic density $\rho(\vec{r})$ determined by normalized multi-electron wave function. Electronic density, compared to wave function, is a physical quantity, which can be measured experimentally by X-ray diffraction. Kohn–Sham equation is the Schrödinger equation of a fictitious system of non-interacting particles that produce the same density as a given system of interacting particles. It is derived by varying the total energy expressed as a functional of $\rho(\vec{r})$. The dependency of electronic energy on $\rho(\vec{r})$ has the following form [7]:

$$U[\rho] = \int V_{\text{ext}}(\vec{r})\rho(\vec{r})d\vec{r} + \frac{1}{2}\int\int \frac{\rho(\vec{r})\rho(\vec{r}')}{|\vec{r}-\vec{r}'|}d\vec{r}d\vec{r}' + U_{\text{k}}[\rho] + U_{xc}[\rho] . \tag{11}$$

Here, the first term describes interaction of electrons with external field incorporating also attraction to nuclei according to Born-Oppenheimer approximation, the second term is Coulomb repulsion of electrons, $U_{\text{k}}[\rho]$ is kinetic energy of known form in Kohn-Sham approach, while $U_{\text{xc}}[\rho]$ is an unknown functional comprising exchange interaction energy and electron correlation as a correction to the SCF approach. Many methods to evaluate $U_{\text{xc}}[\rho]$ have been proposed. The simplest of them is LDA approximation, according to which exchange functional for homogeneous electron gas model has the form

$$U_{\text{x}}^{\text{LDA}}[\rho] = -\frac{3}{4}\left(\frac{3}{\pi}\right)^{1/3}\int\rho^{4/3}(\vec{r})d\vec{r} , \tag{12}$$

while the correlation integrand is a rational approximation fitting exact solutions in limit cases of infinitely weak and infinitely strong correlation. More advanced GGA approximation of $U_{\text{xc}}[\rho]$ takes into account also gradients of electronic density $\vec{\nabla}\rho(\vec{r})$.

Minimization of the functional (11) is carried out using a set of basis functions, linear combinations of which compose molecular orbitals. Methods of the minimization can be figuratively divided by two classes. In methods of the first class, crystal orbitals are approximated by a sum of atomic orbitals centered on each nucleus. Angular components of atomic orbitals are spherical harmonics $Y_{\text{lm}}(\theta,\varphi)$, while radial functions are approximated by analytic functions selected as a basis set. Optimal atomic orbitals should provide correct behavior of electrons near nucleus, as well as far away from them. Most popular basis set is Gaussian-type orbitals having the following form:

$$g(r,\theta,\varphi) \sim r^{n-1}e^{-ar^2}Y_{\text{lm}}(\theta,\varphi) . \tag{13}$$

Here, $r$ is a distance from the given nucleus, $n,l,m$ are principal, azimuthal and magnetic quantum numbers. Despite some disadvantages of Gaussian orbitals, there is a significant advantage, namely, a product of two Gaussian functions centered on two different nuclei is a Gaussian function centered on a line intersecting the nuclei. This fact simplify calculation of Coulomb and exchange integrals. A significant kind of the methods of the first class is a "muffin-tin" (MT) approximation, which consider crystal potential as non-intersecting spheres centered on atoms, so potential is equaled to zero beyond the spheres. Inside MT spheres, solutions of atomic type are constructed, while beyond them wave functions are described by plane waves in such a way, that there was no discontinuity (though the first derivative has it). This method is quite efficient for calculation of elastic constants for many materials [30].

A disadvantage of methods of the first class is a bad convergence of SCF requiring about $10^2$ iterations. In methods of the second class, the solution is initially expanded by plane waves taking into account a symmetry of a crystal. To describe nodal structure of plane waves inside atomic core, it is required about $10^6$ plane waves. To accelerate solution, some approximations are used, such as Orthogonalized Plane Waves (OPW), Augmented Plane Waves (APW), etc. Moreover, for crystals consisting of heavy atoms (i.e. with a big amount of electrons), a

pseudopotential (PSP) method is used. It usually regards only valence electrons, while chemically inactive electrons are united with atomic core resulting in effective potential, which is applicable outside some cutoff radius $r_c$. PSPs are usually prescribed by the most precise calculations, such as relativistic Hartee-Fock method. Plane wave PSP method is realized in ABINIT code.

## 4. Ab initio model used for calculation

We use ABINIT free software for ground state ($T$=0 K) computation mostly by two methods: 1) DFT LDA with Pade approximation of exchange-correlation functional in the form of GTH [31] (reproducing PW [32]) and TM (Troullier-Martins [33]) pseudopotentials generated by A. Khein and D.C. Allan [*www.abinit.org*]; 2) DFT GGA with PBE [34] exchange-correlation functional and ONCV (Optimized Norm-Conserving Vanderbilt [35]) pseudopotentials by D.R. Hamann [36] from ONCVPSP-PBE-PDv0.2 library [*www.abinit.org*]. Compression, tension and shear deformations have been modelled for a cubic cell with 8 atoms, which, in an ideal diamond face-centered cubic structure, have regular tetrahedral neighborhood with the following Bravais coordinates (in units of the lattice parameter, coincide with Cartesian coordinates for undeformed cell): (0,0,0), (1/2,1/2,0), (0,1/2,1/2), (1/2,0,1/2), (1/4,1/4,1/4), (3/4,3/4,1/4), (1/4,3/4,3/4), (3/4,1/4,3/4). When the last four quaternary positions are occupied by another kind of atoms (e.g. by C in SiC), it is called sphalerite or zinc-blende structure. Consideration of the bigger cells having more degrees of freedom unrestricted with periodic conditions, allow to account low-energy transformations on larger scale, which should slightly lower the stress and the elastic limit of crystals.

The accuracy of the reported results is determined by 6×6×6 Monkhorst-Pack [37] computational grid in the reverse *k*-space (shifted by (0.5,0.5,0.5)), and by energy cutoff of plane wave expansions 60 Ha ≈ 1633 eV, that provides a numerical error of the unstrained cell energy less than 0.001 %. ABINIT has effective 3-level parallelization of computations by *k*-points, bands, and fast Fourier transforms, which is suitable for supercomputers. The stress tensor in ABINIT is calculated by Nielsen-Martin formalism [38].

For axial strains along the standard crystallographic axis [100] (Miller notation), the cell has been allowed to change its transverse dimensions, so the Poisson's ratio can be determined. For pure shear strains, a volume of the cell has been optimized. This also secures the applicability of the used pseudopotentials with cutoff radius $r_c$~0.6 Å. Relaxation of atomic positions has been carried out in a process of minimization of the total energy and its gradient [39] by BFGS (Broyden-Fletcher-Goldfarb-Shanno) algorithm until the tolerance $5 \cdot 10^{-5}$ Ha/Bohr ≈ $4 \cdot 10^{-12}$ N on forces is reached. Deformation of a cell with atoms can be performed by two ways: by changing only Bravais vectors without shifting atoms, allowing them to relax to an equilibrium positions, or by changing Bravais vectors with proportional shift of atoms closely to the equilibrium. The first method may "feel" along the deformation path structural instabilities which may be unnoticed by the second method. But the last method has faster relaxation and better convergence of SCF cycles. Since we have quite dense graduation of strain increasing, we have chosen the second way, so the reduced coordinates (relative to cell sides) of atoms instead of Cartesian ones are chosen as initials for each strain step from the last step. However, any kind of metastabilities may be checked with molecular dynamics (MD) [40]. For strained silicon, MD has been calculated by GGA method using Noze-Hoover thermostat [41] at $T$ = 300 K for the time of one atomic oscillation to get representative mean stress.

## 5. Results and discussion

Regarding stress-strain dependencies (Figs. 1-9) obtained by *ab initio* calculations of diamond-like crystals C, SiC, Si, Ge, we will outline some their remarkable features we have observed:

1). First of all, *ab initio* calculations give lattice parameters of the crystals close to experimental values [42], as well as elastic coefficients [46] obtained both by finite strain method and small atomic perturbations method (Tabs. 1 and 3). DFT LDA calculation with TM PSP coincides with DFT GGA with ONCV PSP having a regardless scalar difference in total energy and not big stress overvaluation upon large tension and shear. DFT and GGA exchange-correlation functionals give different signs for small but non-zero piezoelectric coefficient of SiC. Nonetheless, this is a sufficient basis, from which we can proceed to an investigation of nonlinear elastic properties.

Table 1. Lattice parameter $a$ (Å) of the crystals, and elastic constants (GPa, $v$ is dimensionless) with piezoelectric constant $e_{14}$ (C/m$^2$) obtained by response function calculation for small atomic displacements.

|  | $a$ | $c_{11}$ | $c_{12}$ | $c_{44}=G$ | $E_{[100]}$ | $v$ | $e_{14}$ | Method |
|---|---|---|---|---|---|---|---|---|
| C | 3.54 | 1092 | 147 | 588 | 1057 | 0.119 | 0 | 1 |
| C | 3.57 | 1050 | 123 | 559 | 1024 | 0.105 | 0 | 2 |
| C | 3.57 | 1079 | 124 | 578 | 1053 | 0.103 |  | exp [42, 46] |
| SiC | 4.33 | 403 | 142 | 254 | 329 | 0.261 | +0.06 | 1 |
| SiC | 4.38 | 385 | 127 | 242 | 322 | 0.248 | -0.06 | 2 |
| SiC | 4.31 | 409 | 140 | 259 | 338 | 0.255 | 0.01 | 3 |
| SiC | 4.37 | 383 | 125 | 242 | 321 | 0.246 | -0.08 | 4 |
| SiC | 4.35 | 395 | 132 | 236 | 329 | 0.251 |  | exp [43, 47] |
| Si | 5.40 | 161 | 65 | 77 | 124 | 0.288 | 0 | 1 |
| Si | 5.47 | 153 | 57 | 75 | 122 | 0.271 | 0 | 2 |
| Si | 5.43 | 166 | 64 | 80 | 130 | 0.278 |  | exp [44, 48] |
| Ge | 5.53 | 135 | 52 | 67 | 106 | 0.278 | 0 | 1 |
| Ge | 5.65 | 129 | 48 | 67 | 103 | 0.271 |  | exp [45, 49] |

1 – DFT LDA, GTH functional, TM pseudopotentials,
2 – DFT GGA, PBE functional, ONCV pseudopotentials,
3 – DFT LDA with FHI (Fritz-Haber-Institute) pseudopotentials,
4 – DFT GGA with FHI pseudopotentials,
exp – experimental data, 1st ref. to lattice parameter, 2nd ref. to stiffness constants.

2). We explore ~5$^{th}$ order elastic nonlinearity (the order of polynomial approximation of strain energy in Tab. 4) until ultimate strain $\varepsilon_U$ (Tab. 2), at which stress changes its sign, as well as the first derivative of the total energy $U$, so the system tends to another stable phase described by a new local energetic minimum. Although, SiC doesn't exhibit clear change of signs neither for axial (Figs. 3, 5), nor for shear strains (Fig. 8). All examined crystals have the same compressive ultimate strain $\varepsilon_U^c \approx -0.6$, but at high compression beyond $\varepsilon_U^c$ they restore positive stiffness with strong hyperelastic behavior (Fig. 5), while preserving their diamond-like atomic structure in respect to Bravais translations. It is known, that diamond structure may transform to β-Sn or rock salt phases under high hydrostatic (volumetric) pressure [50], but we have not regarded this question for uniaxial stress.

3). At any axial strain, equilibrium positions of atoms remains at their initial reduced coordinates in the basis of Bravais translations. Stress discontinuity and jumps correlate only with Poisson coefficient dependency on strain, i.e. with the cell area associated with the stress. If we allow relaxation from the deformed state, even from the one similar to creep flow beyond $\varepsilon_C^c$ or $\varepsilon_C^t$ (corresponding to flat or lowering stress absolute values), the cell returns during energy

minimization to its initial cubic shape without residual strain. So, formally, the bilinear approximations don't describe elastic-plastic law here, but only nonlinear elasticity, while the limit stress $\sigma_Y$ and strain $\varepsilon_Y$ of linear proportionality usually fit the first stress discontinuity. Real crystals with preexisting defects and big temperature fluctuations happening in large crystal volume, surely, may accumulate plastic strain.

Table 2. Limit true axial $\varepsilon$ and shear $\gamma$ strains with corresponding true stresses $\sigma$ (in GPa): linear proportionality limits (Y), maximal stress limits of bilinear proportionality (C), strength limits (U) – for compression (c), tension (t), or shear (s); see Figs. 1-9.
$h^{s/c,t} = \left| \sqrt{3}\, \sigma_Y^s / \sigma_Y^{c,t} \right|$ – Hill's parameters of assumed anisotropic plasticity.

| | $\varepsilon_Y^c$ | $\varepsilon_C^c$ | $\varepsilon_U^c$ | $\varepsilon_Y^t$ | $\varepsilon_C^t$ | $\varepsilon_U^t$ | $\gamma_Y$ | $\gamma_C$ | $\gamma_U$ | Method |
|---|---|---|---|---|---|---|---|---|---|---|
| Ge | -0.045 | -0.15 | -0.62 | 0.130 | 0.20 | 0.29 | 0.055 | 0.21 | 0.36 | 1 |
| Si | -0.060 | -0.17 | -0.60 | 0.171 | 0.22 | 0.30 | 0.079 | 0.23 | 0.28 | 1 |
| Si | -0.069 | -0.19 | -0.62 | 0.169 | 0.22 | 0.31 | 0.109 | 0.25 | 0.39 | 2 |
| SiC | -0.103 | -0.30 | -0.63 | 0.236 | 0.31 | ~0.47 | 0.180 | 0.31 | ~0.41 | 1 |
| SiC | -0.111 | -0.30 | -0.63 | 0.212 | 0.29 | ~0.47 | 0.171 | 0.32 | ~0.42 | 2 |
| C | -0.165 | -0.27 | -0.62 | 0.189 | 0.33 | 0.52 | 0.226 | 0.35 | 0.40 | 1 |
| C | -0.156 | -0.27 | -0.62 | 0.176 | 0.32 | 0.52 | 0.206 | 0.323 | 0.38 | 2 |
| | $\sigma_Y^c$ | $\sigma_{C,U}^c$ | $h^{s/c}$ | $\sigma_Y^t$ | $\sigma_C^t$ | $h^{s/t}$ | $\sigma_Y^s$ | $\sigma_C^s$ | | |
| Ge | -4.4 | -9.5 | 1.46 | 14.7 | 18.3 | 0.44 | 3.7 | 12.1 | | 1 |
| Si | -6.8 | -11.9 | 1.55 | 24.3 | 28.8 | 0.43 | 6.1 | 15.3 | | 1 |
| Si | -7.7 | -12.7 | 1.84 | 23.1 | 27.0 | 0.61 | 8.2 | 15.7 | | 2 |
| SiC | -27.5 | -49.7 | 2.82 | 91.0 | 98.4 | 0.85 | 44.7 | 65.1 | | 1 |
| SiC | -28.3 | -49.8 | 2.48 | 78.1 | 90.3 | 0.90 | 40.6 | 64.4 | | 2 |
| C | -167.9 | -219.5 | 1.29 | 182.4 | 222.7 | 1.19 | 125.4 | 149.1 | | 1 |
| C | -155.6 | -220.0 | 1.22 | 164.7 | 204.2 | 1.15 | 109.7 | 133.9 | | 2 |

1 – DFT LDA, TM PSP; 2 – DFT GGA, ONCV PSP.

4). Bilinear approximations of stress-strain curves up to $(\varepsilon_C, \sigma_C)$ point in respect to true logarithmic Hencky strain cause considerable difference (for SiC and Si) of approximated Young moduli for tension $E_1^t$, for compression $E_1^c$, and for the limit of small strains $E_0$ (tangent line to the curves at zero strain). One should take this into account when computing large strains or using bilinear model for plasticity in case of early elastic nonlinearity.

5). One can see on Figs. 1-9, that Poisson coefficient is not constant and decreases for a wide interval of axial strains linearly for C and quadratically for SiC, Si, Ge. This decrease have nearly the same rate in the first order $v \approx v_0 - 0.5\varepsilon$ characterizing mostly the crystal geometry than atomic forces. Inconstancy of Poisson coefficient even at small strains should be accounted in common indentation tests for diamond tip as well. At the stretching strain $\varepsilon \approx 0.2$, Poisson coefficient of diamond becomes negative. This is explained by that the atoms in a sublattice of the quaternary positions behaves like an "accordion" structure of other auxetic materials with negative Poisson coefficient [51].

6). For Si and SiC, results (Tab. 2) on maximal tension stress $\sigma_C^t$ and corresponding strain $\varepsilon_C^t$ are close to the results of rod-extension experiment [52] and molecular dynamics studies with Tersoff semi-empirical potential in the same work [52]. For diamond, results on $\sigma_C^t$ and maximal compression stress $\sigma_C^c$ are close to another *ab initio* calculation in [53] (note, that other researchers usually represent engineering strains). Our MD simulation for Si at room

temperature conjugated with DFT GGA calculation of forces results in a bit lower averaged $\sigma_C^t$ (Fig. 2).

Table 3. Approximated from finite strains moduli (in GPa) of elasticity ($E_1$, $G_1$) and tangent moduli of nonlinearity ($E_2$, $G_2$). $E_0$, $G_0$ are obtained from derivative of spline interpolation at zero strain. Polynomial approximations for Poisson coefficient (as relation of logarithmic strains) upon axial true strain $v=v_0+ v_1\varepsilon+ v_2\varepsilon^2$ and relative crystal volume upon shear angular strain $V/V_0=1+v_2\gamma^2+ v_4\gamma^4$.

| | $E_0$ | $E_1^c$ | $E_2^c$ | $E_1^t$ | $E_2^t$ | $v_2$ | $v_4$ | Method |
|---|---|---|---|---|---|---|---|---|
| Ge | 105 | 98 | 48 | 114 | 51 | 0.029 | -3.628 | 1 |
| Si | 124 | 114 | 44 | 142 | 91 | -0.135 | -3.719 | 1 |
| Si | 124 | 111 | 43 | 136 | 77 | -0.051 | -3.761 | 2 |
| SiC | 329 | 266 | 112 | 386 | 99 | 0.334 | - | 1 |
| SiC | 320 | 256 | 113 | 368 | 167 | 0.431 | - | 2 |
| C | 1056 | 1016 | 492 | 965 | 286 | 0.731 | 3.029 | 1 |
| C | 1025 | 1000 | 563 | 935 | 285 | 0.595 | 6.801 | 2 |
| | $G_0$ | $G_1$ | $G_2$ | $\nu_0$ | $\nu_1$ | $\nu_2$ | | |
| Ge | 69 | 68 | 55 | 0.283 | -0.574 | -0.845 | | 1 |
| Si | 77 | 77 | 60 | 0.287 | -0.416 | -0.585 | | 1 |
| Si | 75 | 75 | 54 | 0.271 | -0.450 | -0.616 | | 2 |
| SiC | 253 | 248 | 157 | 0.257 | -0.486 | -0.681 | | 1 |
| SiC | 242 | 238 | 156 | 0.247 | -0.511 | -0.754 | | 2 |
| C | 592 | 599 | 378 | 0.121 | -0.579 | 0.031 | | 1 |
| C | 560 | 532 | 207 | 0.108 | -0.600 | 0.003 | | 2 |

1 – DFT LDA, TM PSP; 2 – DFT GGA, ONCV PSP.

7). Excluding diamond having $\sigma_C^c \approx -\sigma_C^t$ , other crystals (SiC, Si, Ge) have $|\sigma_C^c|$ much less than $\sigma_C^t$. Same goes for limit strains and stresses of linear proportionality ($\varepsilon_Y$, $\sigma_Y$) which we designate as yield limit assuming their scale correlation, since the coincidence of the computed elastic modulus and maximal stress point ($\varepsilon_C$, $\sigma_C$) with experimental values give minor differences with experimental stress-strain curve to fit yield point with bilinear law. So the conclusion about plastic axial anisotropy can be made. Moreover, shear limit stress of linear proportionality $\sigma_Y^s$ doesn't satisfy the condition of plastic isotropy as well, that is demonstrated with the Hill's parameters $h$ (Tab. 2) and surfaces (Fig. 10).

8). Unlike axial deformation, the shear deformation in $(\vec{b}_1, \vec{b}_2)$ plane cause changing of $b_3$-components of the atomic reduced coordinates in Bravais basis, while $b_1$ and $b_2$ components remain the same. Upon shear deformation, atoms in quaternary positions tends to the cell planes, and only diamond successfully introduce them there in line chains at ultimate shear strain $\gamma_U \approx 0.39 \approx 22°$, while fracturing, i.e. transforming into compliant one-face-centered orthorhombic structure with doubled volume and Bravais coordinates of the considered cell atoms (0, 0, -1/8), (1/2, 1/2, -1/8), (0, 1/2, 3/8), (1/2, 0, 3/8), (1/4, 1/4, 3/8), (3/4, 3/4, 3/4), (1/4, 3/4, 5/8), (3/4, 1/4, 5/8).

9). Despite of the similar way of atomic relaxation, pure shear deformation causes volume expansion for C and SiC, but contraction for Si and Ge. The dependency of the cell volume (related to undeformed cell volume) has been approximated with quadratic or biquadratic polynoms (Fig. 6-9, Tab. 3).

Table 4. Polynomial approximation of the cell total energy on strain in the anharmonic range having continuous differentiability. $U/|U_0| = -1 + u_2\varepsilon^2 + u_3\varepsilon^3 + u_4\varepsilon^4 + u_5\varepsilon^5$, where it is engineering strain $\varepsilon = \Delta L/L_0$ for axial deformation (the energy is redrawn in logarithmic strains on Figs. 1-9).

|      | strain | $U_0$ (eV) | $u_2$ | $u_3$ | $u_4$ | $u_5$ | Method |
|------|--------|--------|--------|---------|---------|---------|--------|
| Ge   | axial  | -1101.30 | 0.0446 | 0.0452  | -0.1470 | -0.2580 | 1 |
| Ge   | shear  | -1101.30 | 0.0285 | 0.0280  | -0.0326 | -0.3315 | 1 |
| Si   | axial  | -966.24  | 0.0602 | 0.0673  | -0.1751 | -0.3185 | 1 |
| Si   | axial  | -921.24  | 0.0642 | 0.0585  | -0.1690 | -0.2544 | 2 |
| Si   | shear  | -966.24  | 0.0445 | -0.1109 | 0.5904  | -1.1508 | 1 |
| Si   | shear  | -921.24  | 0.0465 | -0.0966 | 0.5421  | -1.0852 | 2 |
| SiC  | axial  | -1142.80 | 0.0699 | 0.0496  | -0.0675 | -0.1811 | 1 |
| SiC  | axial  | -1117.93 | 0.0720 | 0.0466  | -0.0749 | -0.1897 | 2 |
| SiC  | shear  | -1142.80 | 0.0577 | -0.0166 | 0.0963  | -0.1926 | 1 |
| SiC  | shear  | -1117.93 | 0.0607 | -0.0524 | 0.2437  | -0.3729 | 2 |
| C    | axial  | -1314.55 | 0.1107 | -0.0443 | -0.1189 | 0.0859  | 1 |
| C    | axial  | -1310.27 | 0.1105 | -0.0489 | -0.1218 | 0.0947  | 2 |
| C    | shear  | -1314.55 | 0.0639 | -0.0303 | 0.1668  | -0.2652 | 1 |
| C    | shear  | -1310.27 | 0.0621 | -0.0230 | 0.1368  | -0.2436 | 2 |

1 – DFT LDA, TM PSP, 2 – DFT GGA, ONCV PSP.

**References**

[1] R. Ghodssi, P. Lin, *MEMS Materials and Processes Handbook* (Springer, Berlin, 2011).
[2] T. Polster, M. Hoffman // *Procedia Chemistry* **1(1)** (2009) 144.
[3] A.C. Fisher-Crips, *Nanoindentation* (Springer, Berlin, 2011).
[4] R.A. Evarestov, *Quantum Chemistry of Solids* (Springer, Berlin, 2012).
[5] C.J. Cramer. *Essentials of Computational Chemistry* (J. Wiley & Sons, Chichester, 2004).
[6] D.B. Cook, *Handbook of Computational Quantum Chemistry* (Oxford University Press, Oxford, 1998).
[7] T. Tsuneda, *Density Functional Theory in Quantum Chemistry* (Springer, Tokyo, 2014).
[8] D. Sholl, J.A. Steckel, *Density Functional Theory: a Practical Introduction* (John Wiley & Sons, Hoboken, 2009).
[9] X. Gonze, B. Amadon, P.-M. Anglade, J.-M. Beuken, F. Bottin, P. Boulanger, F. Bruneval, D. Caliste[j], R. Caracas, M. Côté, T. Deutsch, L. Genovese, Ph. Ghosez, M. Giantomassi, S. Goedecker, D.R. Hamann, P. Hermet, F. Jollet, G. Jomard, S. Leroux, M. Mancini, S. Mazevet, M.J.T. Oliveira, G. Onida, Y. Pouillon, T. Rangel, G.-M. Rignanese, D. Sangalli, R. Shaltaf, M. Torrent, M.J. Verstraete, G. Zerah, J.W. Zwanziger // *Computer Physics Communications* **180** (2009) 2582.
[10] J.F. Nye, *Physical Properties of Crystals: Their Representation by Tensors and Matrices* (Oxford University Press, Oxford, 1957).
[11] F.D. Murnaghan, *Finite Deformation of an Elastic Solid* (John Wiley & Sons, New York, 1951).
[12] A.E. Green, J.E. Adkins, *Large Elastic Deformations and Non-Linear Continuum Mechanics* (Clarendon Press, Oxford, 1960).

[13] A.I. Lurie, *Non-linear Theory of Elasticity* (North-Holland, Amsterdam, 1990).

[14] R.N. Thurston, K. Brugger // *Physical Review* **133** (1964) A1604.

[15] L.K. Zarembo, V.A. Krasil'nikov // *Soviet Physics-Uspekhi* **13** (1971) 778.

[16] O.H. Nielsen, R.M. Martin // *Physical Review B* **32** (1985) 3792.

[17] E.A. de Souza Neto, D. Perić, D.R.J. Owen, *Computational Methods for Plasticity: Theory and Applications* (John Wiley & Sons, Chichester, 2008).

[18] X. Gonze, C. Lee // *Physical Review B* **55** (1997) 10355.

[19] S. Baroni, S. de Gironcoli, A. Dal Corso, P. Giannozzi // *Reviews of Modern Physics* **73** (2001) 515.

[20] V.K. Tewary // *Advances in Physics* **22** (1973) 757.

[21] L.M. Kachanov, *Foundations of the Theory of Plasticity* (North-Holland, Amsterdam, 1971).

[22] K. Hashiguchi, Y. Yamakawa, *Introduction to Finite Strain Theory for Continuum Elasto-Plasticity* (John Wiley & Sons, Chichester, 2012).

[23] R. Hill, *The Mathematical Theory of Plasticity* (Clarendon Press, Oxford, 1950).

[24] M.Yu. Gutkin, I.A. Ovid'ko, *Plastic Deformation in Nanocrystalline Materials* (Springer-Verlag, Berlin Heidelberg, 2004).

[25] I.A. Ovid'ko // *Applied Physics Letters* **99** (2011) 061907.

[26] L.M. Zubov, *Nonlinear Theory of Dislocations and Disclinations in Elastic Bodies* (Springer-Verlag, Berlin Heidelberg, 1997).

[27] R. Hill // *Proceedings of the Royal Society of London* **193** (1948) 281.

[28] R. Hill // *Mathematical Proceedings of the Cambridge Philosophical Society* **85** (1979) 179.

[29] C.F. Shih, D. Lee // *Journal of Engineering Materials and Technology* **100** (1978) 294.

[30] E. Konstantinova, M.J.V. Bell, V. Anjos // *Intermetallics* **16** (2008) 1040.

[31] S. Goedecker, M. Teter, J. Hutter // *Physical Review B* **54** (1996) 1703.

[32] J.P. Perdew, Y. Wang // *Physical Review B* **45** (1992) 13244.

[33] N. Troullier, J.L. Martins // *Physical Review B* **43** (1991) 1993.

[34] J.P. Perdew, K. Burke, M. Ernzerhof // *Physical Review Letters* **77** (1996) 3865.

[35] D. Vanderbilt // *Physical Review B* **41** (1990) 7892.

[36] D.R. Hamann // *Physical Review B* **88** (2013) 085117.

[37] H.J. Monkhorst, J.D. Pack // *Physical Review B* **13(11)** (1976) 5188.

[38] O.H. Nielsen, R.M. Martin // *Physical Review B* **32** (1985) 3780.

[39] H.B. Schlegel // *Journal of Computational Chemistry* **3** (1982) 214.

[40] D. Marx, J. Hutter, *Ab Initio Molecular Dynamics: Basic Theory and Advanced Methods* (Cambridge University Press, Cambridge, 2009).

[41] S. Nosé // *Journal of Chemical Physics* **81** (1984) 511.

[42] S. Stoupin, Y.V. Shvyd'ko // *Physical Review Letters* **104** (2010) 085901.

[43] Z. Li, R.C. Bradt // *Journal of Materials Science* **21** (1986) 4366.

[44] W.M. Yim, R.J. Paff // *Journal of Applied Physics* **45** (1974) 1456.

[45] M.E. Straumanis, E.Z. Aka // *Journal of Applied Physics* **23** (1952) 330.

[46] H.J. McSkimin, P. Andreatch // *Journal of Applied Physics* **43** (1972) 2944.

[47] G.F. Dirras, P. Djemia, Y. Roussigné, K.M. Jackson // *Materials Science & Engineering A* **387–389** (2004) 302.

[48] H.J. McSkimin // *Journal of Applied Physics* **24** (1953) 988.

[49] H.J. McSkimin, P. Andreatch // *Journal of Applied Physics* **34** (1963) 651.

[50] J.R. Chelikowsky // *Physical Review B* **35** (1987) 1174.

[51] K.E. Evans // *Endeavour* **15(4)** (1991) 170.

[52] V.I. Ivashchenko, P.E.A. Turchi, V.I. Shevchenko // *Physical Review B* **75** (2007) 085209.

[53] X. Luo, Zh. Liu, B. Xu, D. Yu, Y. Tian, H.-T. Wang, J. He // *The Journal of Physical Chemistry C* **114** (2010) 17851.